Open access • Journal Article • DOI:10.1002/ANIE.201706463

Role of the adsorbed oxygen species in the selective electrochemical reduction of CO2 to alcohols and carbonyls on copper electrodes — Source link

Cécile S. Le Duff, Matthew J. Lawrence, Paramaconi Rodriguez

Institutions: University of Birmingham

Published on: 09 Oct 2017 - Angewandte Chemie (Angew Chem Int Ed Engl)

Topics: Cyclic voltammetry, Voltammetry, Electrochemistry and Selectivity

Role of the adsorbed oxygen species in the selective electrochemical reduction of CO2 to alcohols and carbonyls on copper electrodes

Rodriguez, Paramaconi; Lawrence, Matthew; Le Duff, Cécile

DOI:
10.1002/anie.201706463

Document Version
Peer reviewed version

Citation for published version (Harvard):
Rodriguez, P, Lawrence, M & Le Duff, C 2017, 'Role of the adsorbed oxygen species in the selective electrochemical reduction of CO2 to alcohols and carbonyls on copper electrodes', *Angewandte Chemie (International Edition)* , vol. 56, no. 42, pp. 12919–12924. https://doi.org/10.1002/anie.201706463

Role of the adsorbed oxygen species in the selective electrochemical reduction of CO_2 to alcohols and carbonyls on copper electrodes

Cécile S. Le Duff, Matthew J. Lawrence and Paramaconi Rodriguez[a]

Abstract: The electrochemical reduction of CO_2 into fuels has gained significant attention recently as source of renewable carbon-based fuels. The unique high selectivity of copper in the electrochemical reduction of CO_2 to hydrocarbons has called much interest in discovering its mechanism. In order to provide significant information about the role of oxygen in the electrochemical reduction of CO_2 on Cu electrodes, the conditions of the surface structure and the composition of the Cu single crystal electrodes were controlled over time. This was achieved using pulsed voltammetry, since the pulse sequence can be programmed to guarantee reproducible initial conditions for the reaction at every fraction of time and at a given frequency. In contrast to the selectivity of CO_2 reduction using cyclic voltammetry and chronoamperometric methods, a large selection of oxygenated hydrocarbons was found under alternating voltage conditions. Product selectivity towards the formation of oxygenated hydrocarbon was associated to the coverage of oxygen species, which is surface-structure-and-potential dependent.

Recycling of CO_2 into fuels is a promising way to address the challenge of reducing the CO_2 emissions that contribute to global warming. The electrochemical conversion of CO_2 into fuels is one of the most promising paths towards the realisation of a sustainable fuel economy because it can be powered by renewable sources (e.g., solar, wind, tidal, etc.). To date, copper and copper oxide-derived surfaces are the only catalysts that can electrochemically convert CO_2 to high value and energy-dense products such as methane, ethylene, formic acid, methanol and ethanol, among others;[1] however, the efficiency and the selectivity of these catalysts are far from optimal and the parameters controlling these factors are not-fully understood. Such differences in reactivity and selectivity have been attributed to the surface area, particle size, surface structure, roughness of the electrode and even to the history of the electrode.[1a, 1e, 2]

Some understanding of the surface structure reactivity and selectivity relationship for the CO_2 electrochemical reduction reaction has been gained from theoretical and experimental data on copper single-crystal electrodes.[1a, 1d, 3] It has been reported that on Cu (111) facets, the formation of methane is favoured; whereas, ethylene formation is predominant on Cu(100) surfaces.[1a] Although these studies provide an important insight into the mechanism of the CO_2 reduction reaction and into some of the parameters affecting the catalytic activity, they have not been able to provide an explanation of the broad product distribution found on Cu nanocatalysts. A possible explanation to the diverse selectivity is the dynamic nature of the structure of copper surfaces under CO_2 electrochemical reduction conditions.[4]

Recently, it has been noted that the effect of the role of oxygen content on the copper catalyst also adds complexity to the system.[1e, 1f, 5] Some reports have claimed the formation of methanol during CO_2 reduction on Cu_2O electrodes with faradaic efficiencies (FE) of 38 %.[2a, 6] On the other hand, in a similar system – Cu_2O films – others have reported the formation of CO (FE ~ 45 %), formic acid (FE 30 %), ethanol (FE~ 4.7 %) and ethylene (FE~93.9 %), but no methanol.[1f] Kas *et al*. reported the formation of formic acid as the only liquid product (FE 20 %) during CO_2 reduction on Cu_2O prepared by electrochemical oxidation of copper electrodes.[1e] The causes of the different selectivity have been ascribed to a myriad of factors such as the oxidation state of the Cu, oxygen content on the films and the roughness of the electrode (surface structure). The origin of the different selectivity remains a mystery and its elucidation would impact significantly on the development of improved catalysts for the CO_2 reduction.

In order to provide significant information of the role of oxygen in the electrochemical reduction of CO_2 on Cu electrodes, one turns to simple experiments which allow more control over the experimental conditions and, therefore, allow the separation of the parameters that influence the selectivity. In order for such an enterprise to be achieved, we have utilised Cu single crystal electrodes with crystal structure (100) and (111) and an electrochemical strategy to control the oxygen content at the surface. The surface structure and the composition of the single crystal electrodes were controlled over time. This was achieved using pulsed voltammetry,[7] since the pulse sequence can be programmed to guarantee reproducible initial conditions for the reaction (Figure 1A) at every fraction of time and at a given frequency.

A short pulse at high potential (-0.2, -0.25, - 0.3 or -0.35 V vs RHE) was superimposed onto a normal voltammetry cycle to periodically recover the initial reaction conditions. These short pulses resulted in the co-adsorption of anions and hydroxide species onto the copper electrodes.[8] They may also favour the desorption/oxidation of the accumulated adsorbed intermediates. In addition, they may avoid possible structural changes associated to H_2 brightening at negative potentials.

Figure 2 shows the pulsed voltammetry of the Cu(111) and Cu(100) electrodes in a phosphate buffer solution at pH=7.9±0.1, in both the presence and absence of CO_2 in the solution. As indicated in the figure, each of the curves corresponds to different upper potential pulses. The cyclic voltammetry under the same conditions for each electrode was included for comparison. As can be seen in the cyclic voltammetry on the inset of Figure 2A, the selected potential for the positive step occurred in the region where the co-adsorption of phosphates and OH species took place.[8b] At higher potentials, the formation of Cu oxides and dissolution of copper resulted in

[a] Dr. Cecile S. Le Duff, Matthew J. Lawrence, Dr. Paramaconi Rodriguez
School of Chemistry
University of Birmingham
Edgbaston, Birmingham, B15 2TT, United Kingdom
E-mail: p.b.rodriguez@bham.ac.uk

Supporting information for this article is given via a link at the end of the document.

changes of the surface structure and an increase of the step-density.[8b, 9]

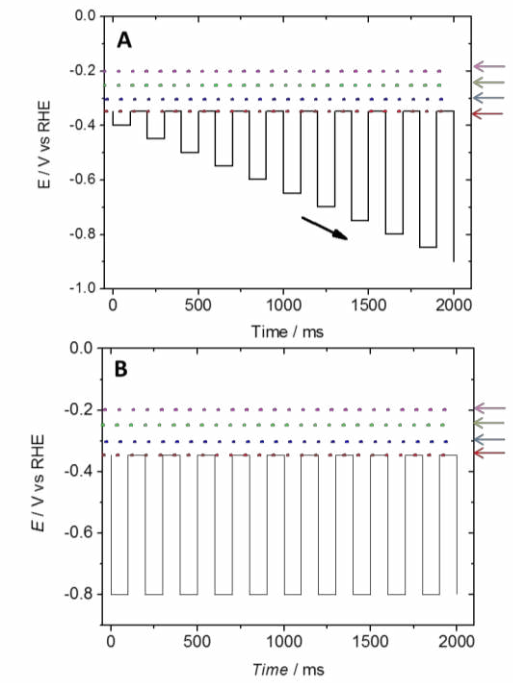

Figure 1. (A) Pulse program for the pulsed voltammetry and (B) alternate voltage electrolysis program. The coloured lines indicate the different positive step potentials. Both the pulse time and pulse interval used during the pulse voltammetry were 0.1 s; alternate voltage electrolysis was performed with a frequency of 10 Hz over 60 minutes.

In both cases, Cu(111) and Cu(100), the pulse voltammetry in the absence of CO_2 showed larger current contributions between -0.5 V and -0.8 V, in comparison with the cyclic voltammetry. In this potential window, the voltammetry of Cu(111) showed a peak at -0.55 V, which shifted towards more positive potentials when the pulse at the higher potentials became more positive. In addition, the total change of the process in the given potential region increased. The pulse voltammetries also showed a shift of the onset of hydrogen evolution reaction towards more negative potentials and showed a clear change on the reaction rate.

The blank pulse voltammetries of Cu(100) showed similar behaviour to that described for Cu(111); however, differences in the peak position can be perceived. In the case of Cu(100), a broader peak appears at a more negative potential of -0.70 V vs RHE. The hydrogen evolution reaction is also shifted towards more negative potentials.

In the presence of a CO_2 saturated solution (Figures 2B and 2D), the faraday currents associated to the reduction of CO_2 are significantly larger than in the cyclic voltammetries. A representative set of transients, recorded for the Cu(111) and Cu(100) electrodes during the pulsed voltammetry experiments, are shown in Figure S3. The two processes observed in the blank voltammetries can also be distinguished in the presence of CO_2; the current, in the presence of CO_2, is larger than the currents in the absence of CO_2, even at low potentials (see the comparison in Figure S2). This suggests that, under pulse voltammetry conditions, Cu electrodes are capable of reducing CO_2 at potentials as low as -0.4 V vs RHE. The larger currents of the pulsed voltammetry, in comparison with the cyclic voltammetry, are observed in the potential region between 0 V and 1.2 V. At higher potentials, the current densities of both types of voltammetries are similar.

One objective of this work was to separate the different parameters that contribute to the product selectivity during CO_2 reduction on copper electrodes, as a function of potential. In order to confirm the stability of the surface under pulse voltammetry conditions, we have recorded the blank voltammetry of the single crystal electrodes in NaOH before and after each pulse voltammetry. It has been previously reported that the cyclic voltammetry of Cu single crystal electrodes in NaOH is sensitive to the presence of structural changes.[10] As can be seen in Figures S3 and S4, the blank voltammetries of Cu(111) and Cu(100) in NaOH are in agreement with previous results. Our results do not show any significant structural changes after the step potential protocol, neither in the absence nor the presence of CO_2, when the step potential is kept below -0.25 V vs RHE. When the step potential on the pulse voltammetry was as high as -0.2 V vs RHE, significant changes in the voltammetries were observed. There are most likely associated to changes in the microrugosity of the surface which can be associated to the lattice expansion of the copper due to the formation of copper oxides and to the copper dissolution.[7-8] Therefore, in order to eliminate the effect of changes of the structure, the product characterization is reported only for the step potentials at -0.35 V, -0.3 V and -0.25 V vs RHE.

The product selectivity for CO_2 reduction on Cu(111) and Cu(100), as determined by on-line electrochemical mass spectrometry (OLEMS), during pulse voltammetry, is shown in Figure 3.

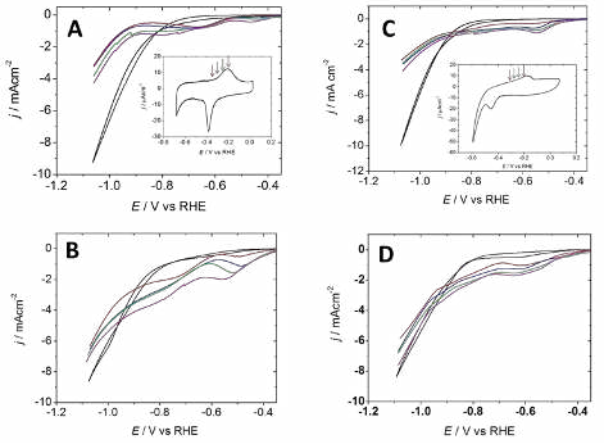

Figure 2. Pulse voltammetries of Cu(100) (left column) and Cu(111) (right column) electrodes in phosphate buffer solution. (A) and (C) show the blank voltammetries in the absence of CO_2; (C) and (D) show the voltammetries in the presence of CO_2. The black curves correspond to cyclic voltammetries, taken at (υ=10 mV/s), in the absence and presence of CO_2. The inset correspond to the cyclic voltammetries of the Cu(111) and Cu(100) in the absence of CO_2 (υ=50 mV/s). The arrows indicate the positive potential steps during the pulse voltammetries.

The product distribution of the gaseous species from the cyclic voltammetries are also included for comparison. As can be seen, the formation of hydrogen (m/z=2) under the pulse potential program is significantly compromised in both single-crystal electrodes when compared with the hydrogen formation during the cyclic voltammetry. In fact, as indicated by the arrows, the hydrogen production decreases as the pulse potential becomes less negative. Similar to the product distribution of CO_2 reduction using cyclic voltammetry,[1a] the formation of methane (m/z=15) and ethylene (m/z=26) produced under pulse potential voltammetry also depends on the surface structure and on the applied potential. On Cu(111), the formation of CH_4 and C_2H_4 under the pulse potential voltammetries program takes place at higher overpotentials when compared with cyclic voltammetry. In addition, the production of CH_4 and C_2H_4 decreases as the pulse potential becomes less negative. This is associated to the decrease in the coverage of the protons at the negative step potentials which occurs due to an increase in the coverage of the oxide species at the upper step potential. As previously reported, it was observed in the cyclic voltammetries that Cu(100) is more selective toward the formation of C_2H_4, in comparison to the formation of CH_4, at low overpotentials. Under step potential conditions, the formation of C_2H_4 and H_2 on Cu(100) decreases as the upper step potential becomes more positive. At the upper step potential of -0.2 V, the formation of C_2H_4 is almost negligible. This can be associated to the suppression of protons adsorbed during the step potential regime. Surprisingly, the electrochemical reduction of CO_2 on Cu(100) shows a significant increase in the production of CH_4 at potentials between -0.7 V and 1.2 V vs RHE, when the step potential is applied. A maximum rate of production of CH_4 species was observed between -0.8 V and -1.0 V vs RHE when the upper potentials were stepped at -0.3 V and -0.35 V vs RHE. It is important to note that the potential at which the maximum formation rate of CH_4 appears (-0.9 V vs RHE) coincides with the potential of the crossover of the cyclic voltammetry curve and the curve of the pulse voltammetries for CO_2 reduction and at the potential at which the formation of H_2 increases. In addition, at this potential, a change in the Tafel slope of the pulse voltammetries can be distinguished. Currently, we postulate that this might be associated with the coverage, adsorbate geometries and available adsorption sites. In addition to the well-known gaseous product reported by electrochemical mass spectroscopy, m/z=31, presumably associated to the formation of methanol, was also detected. Surprisingly, signals of m/z=31 were observed in both electrodes, Cu(111) and Cu(100), during pulse voltammetries at potentials as low as -0.6 V vs RHE. These signals were observed only under pulse potential conditions when the pulse potentials were -0.3 and -0.25. In both cases, the amount of the fragment m/z=31 increased when the pulse potential increased from -0.35 V to -0.3 V vs RHE; however, the signals of m/z=31 were not observed during the cyclic voltammetries, nor during the pulse voltammetry with pulse potential -0.25. Although m/z=31 might be associated to the fragment CH_3OH^+ of methanol, it might be also attributed to fragments of other products reported for the CO_2 reduction on copper electrodes (e.g., ethanol).[4b] Further insights into the mechanism will be presented below, after the analysis of the liquid products by NMR.

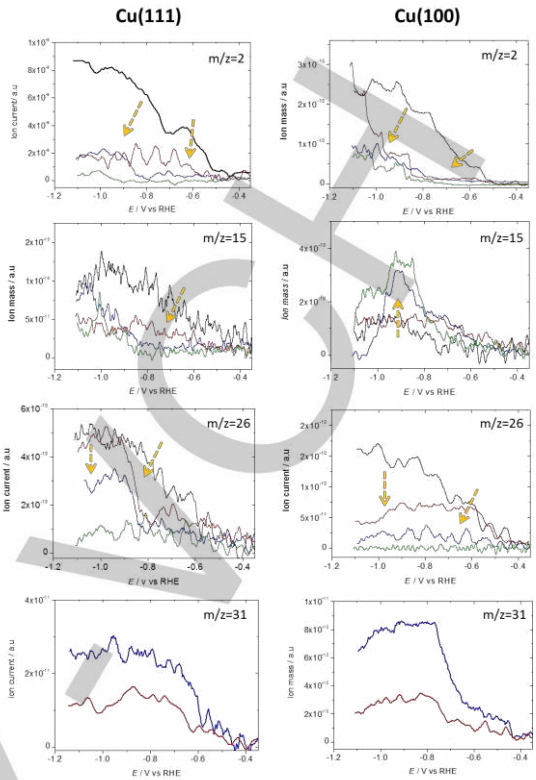

Figure 3. Volatile products with m/z=2, m/z=15, m/z=26 and m/z=31, probed by OLEMS during the reduction of CO_2 on Cu(111) and Cu(100) electrodes. The black line corresponds to the volatile products formed during a cathodic scan of one cyclic voltammetry. The green line, blue line and red line correspond to the volatile products detected during the pulse voltammetries at -0.25 V, -0.3 V and -0.35 V, respectively. The orange arrows indicate, for the different products, the trends observed, as functions of the upper limit potential.

In order to identify the liquid products during the electrochemical reduction of CO_2 under step potential conditions, we have performed long term experiments in an electrochemical cell with reduced volume, as described in the experimental section and in Figure S1. The experiments were performed by applying a square wave potential with frequency of 10 Hz between -0.8 V vs RHE and the positive potentials of -0.25 V, -0.3 V and -0.35 V vs RHE, as indicated in Figure 1B. The experiments were performed during 1 h and 800 μL samples were collected every 15 min and analysed by 1H NMR, as described in the experimental section and supporting information. Figures S6-S9 show the 1H NMR characterisation of the products of the CO_2 reduction after the square wave potential protocol for the step potentials at -0.3 V and -0.25 V. Table 1 summarises the products observed under these experimental conditions. Cyclic voltammetries of both electrodes, before and after the electrolysis, were recorded and confirm the stability of the surface structure of the electrodes under these conditions (Figure S10). The small changes observed in the blank voltammetries of Cu(111) and Cu(100) in Figure S10 can be associated to small changes in the surface structure (i.e., the formation of steps and kinks) or to the presence of adsorbed species generated during electrolysis.

Previous works, using video scan rate in-situ STM, by Matsushima et al. have shown that hydrogen induces reconstruction of Cu(100) from a (1x1) unit cell to a c(p×8) unit cell.[11] However, no reconstruction was found at pH 3, nor higher. The authors have also reported that this reconstruction process is reversible.

On the other hand, Soriaga's group reported that, in alkaline media, a copper polycrystalline electrode undergoes reconstruction during hydrogen evolution conditions.[4] This slow, sequential transformation showed first the formation of a Cu(111) phase followed by the formation of Cu(100).

As can be seen on Table 1, a larger selection of oxygenated hydrocarbons was found under alternate voltage conditions than under DC chronoamperometric conditions.[2g, 4a] Interestingly, the product selectivity towards C1, C2 and C3 oxygenated hydrocarbons as a function of the surface structure was also observed under the alternate voltage conditions.

Table 1. Liquid products probed by 1H NMR during CO_2 reduction under the alternate voltage electrolysis with a frequency 10 Hz. [compound] is present in traces; compound is most intense peak.

Surface structure	Electrolysis time	Applied potential	
		-0.8 V to -0.3 V	-0.8 V to -0.25 V
Cu(100)	30 min	C1: $\underline{CH_3OH}$ C2: CH_3CH_2OH C3: $(CH_3)_2CO$	C1: CH_3OH C3: $\underline{(CH_3)_2CO}$
	60 min	C1: $HCOO^-$ C2: $\underline{CH_3CH_2OH}$ C3: $(CH_3)_2CO$	C1: $HCOO^-$, CH_3OH C2: CH_3CH_2OH C3: $\underline{(CH_3)_2CO}$
Cu(111)	30 min	C1: $\underline{CH_3OH}$ C3: $[(CH_3)_2CO]$	C1: $[HCOO^-]$, $\underline{CH_3OH}$
	60 min	C1: $HCOO^-$, $\underline{CH_3OH}$	C1: $HCOO^-$, $\underline{CH_3OH}$ C2: $[CH_3COO^-]$

The C2 and C3 oxygenated products – ethanol, acetaldehyde and acetone – were observed only on Cu(100); whereas, C1 oxygenated products – formic acid and methanol – were formed on both surface structures. Other products, such as acetaldehyde and acetate, were observed at step potentials more positive than -0.2 V; however, significant changes in the surface structure were observed after the electrolysis (see Figure S11); therefore, changes in the selectivity could be associated to uncontrolled factors during the electrolysis. Under these experimental conditions, no other C3-C4 products previously reported for the CO_2 reduction on copper electrodes were detected.[12]

It has been proposed, in the literature, that carbon monoxide is the common intermediate in the formation, during the CO_2 reduction, of a wide variety of products, such as CH_4, CH_3OH and C_2H_4. During CO_2 reduction, the adsorbed carbon monoxide is formed first ($2e^-/2H^+$), followed by the formation of an adsorbed carbonyl species, such as (CHO_{ads}) or (COH_{ads}).[13] These intermediates later react to form methane and/or methanol through an electron-proton transfer, as described in Equation (I) or Equation (II):

$$(COH_{ads}) \text{ or } (CHO_{ads}) + 5e^- + 5H^+ \rightarrow CH_4 + H_2O \quad (I)$$

$$(COH_{ads}) \text{ or } (CHO_{ads}) + 3e^- + 3H^+ \rightarrow CH_3OH \quad (II)$$

The decrease in the formation of H_2 on both electrodes and the decrease in the formation of CH_4 on Cu(111) (as observed in the OLEMS under step potential conditions) can both be attributed to the decrease of the H^+ adsorption due to the presence of OH adsorbed as induced at the most positive step potential. The appearance of methanol or ethanol (m/z=32 in the OLEMS experiments) is consistent with the decrease of hydrogen coverage (as given by the stoichiometry in Eq. II vs Eq. I).

On the other hand, ethylene is formed by dimerization of intermediate species through a 6 electron-proton transfer according to Equation (III):

$$2(COH_{ads}) \text{ or } 2(CHO_{ads}) + 6e^- + 6H^+ \rightarrow C_2H_4 + 2H_2O \quad (III)$$

If the reaction mechanism follows a Langmuir-Hinshelwood mechanism, such coupling reaction requires the presence of two adjacent C-containing adsorbates. The proximity of the reactants will be given by the surface coverage and the surface structure of the adsorbate species (e.g., surface oxides, phosphate anions and reactive intermediates); therefore, the formation of C_2H_4 must be driven by an increase in the surface concentration of C-containing adsorbate, to the detriment of proton adsorption.

The presence of alcohols and ketones in the C2 and C3 products indicates that the C–C coupling might occur before at least one of the two carbon-oxygen bonds in CO_2 is broken, accompanied or followed by hydrogenation reactions. The increase of CO_{ads} and COH_{ads} species on the surface, together with the decrease of the hydrogen availability on the surface, are expected; the coupling of $CH_{x\ ads}$ and CO_{ads} or COH_{ads} species results in the formation of terminal alcohols and ketones.

After 60 minutes of electrolysis, it was observed that formic acid was a major product. Previous studies proposed that the mechanistic pathway toward formic acid formation is independent from the formation of carbon monoxide, and that formic acid cannot be further reduced to other products. It was assumed, therefore, that the appearance of formic acid must be associated to a change in the reaction mechanism over the course of the reaction. It has also been shown that the formation of formic acid and formate is favoured under alkaline conditions. Therefore, our observation of the formation of formic acid is consistent with a change of pH due to the consumption of protons during the electrolysis. Despite the use of a buffer solution, during the electrolysis, small changes of pH (from pH=7.9 to pH=8.2 after 30 minutes and pH=8.6 after 1 hour) were measured in the solution; these might result in small changes in the selectivity.

Our results confirm that selectivity toward the formation of C1, C2 and C3 products strongly depends on the geometry of the copper surface; C2 and C3 products are more likely to form on Cu(100) than on Cu(111). The formation of oxygenated species – formate, methanol, ethanol, acetone and acetaldehyde – is not necessarily linked to the surface structure, nor to the roughness of the surface. The formation of oxygenated hydrocarbon may be associated to the adsorption of OH species to the surface when the potential is stepped to the upper potential. It has been

proposed that the promotion of CO_2 chemisorbed on oxygen-modified Cu surfaces, and the subsequent hydrogenation, is a key feature of the mechanism in the reduction of CO_2 to methanol.[14] Early work from Bowker reported the surface structure sensitivity and the effect of the pre-dose oxygen species in the formation of different intermediates in the gas phase. Methoxy species (CH_3O) are formed when dosing methanol onto Cu(110). On the other hand, dosing methanol onto a partially oxidised Cu(110) produced a formate species.[15] A recent work has revealed the importance of copper suboxide and the critical role of water in the first step of activation of CO_2 on a Cu(111) surface in the gas phase.[16]

Product selectivity should be associated to OH coverage, which is surface structure and potential dependent. Friebel *et al.* reported that, at potentials close to the onset of anodic dissolution/oxide growth of Cu(111), sulfate and water co-adsorb to form a hexagonal superstructure with a (13×13) R13.9° unit cell.[7a] Similarities in structure are expected on the phosphate, given the nature of the anion. In the case of the Cu(100), Cruickshank *et al.* reported the formation, in a diluted solution of $HClO_4$ and H_2SO_4, of a $\sqrt{2}x\sqrt{2}$ R45° structure associated to the adsorption of either oxygen or OH on the (100) surface.[17] However, it is important to mention that later results by Vogt *et al.* suggested that such surface structure of the adlayer is influenced by the presence of chloride contaminants in the electrolyte.[18]

Until now, the electrochemical approaches did not allow for control over the surface coverage of an oxygen specie during an experiment. Linear voltammetries or chronoamperometric techniques are not appropriate techniques since the Cu-oxides (O and OH species) depend on the electrode potential, the direction of the scan and the previous history of the electrode. In this report, we have demonstrated that conditions can be controlled over time. This is achieved by using Cu single crystal electrodes, pulsed voltammetry and the AC electrolysis because the pulse potential sequence can be tuned to ensure reproducible initial conditions without compromising the surface structure (S4-5 and S10).

We propose here that the decrease of H_2 availability for the hydrogenation reaction results in the formation of C-C bonds and of oxygenated products, and that the selectivity of the oxygenated products is related to the surface coverage of OH on the different surface structures. Further tuning of the product selectivity can be achieved, not only by changing parameters in the pulse program (such as potential window, frequency, duty cycle and AC offset), but also by changing the surface coverage of the OH specie. The different OH coverage can be tweaked though anion adsorption, non-covalent interaction or pH.[19] Even though it was not the main subject of this work, it could also be concluded that the cooperativity effect between CO_{ads} and OH_{ads} could be playing a role in the reaction mechanism, similar to that which has been reported for gold electrodes.[20]

In addition, this work opens the door to elucidate the effects of oxide supports and promoters on the activity and selectivity of supported Cu NPs and Cu thin-films in the conversion of CO_2 into high added-value molecules.

Experimental Section

Two sets of electrochemical cells were used in the experiments (see SI). In all the experiments, a gold wire was used as a counter electrode and a Hg/HgO electrode was used as a reference electrode. All the graphs are presented in reversible hydrogen electrode (RHE) scale. Electrochemical measurements were performed with an Autolab PGSTAT12. The phosphate buffer solution (pH=7.9; 94 mL of 1 M K_2HPO_4 + 6 mL of 1 M KH_2PO_4) was prepared from Sigma-Aldrich ACS reagent chemicals (>98% and >99.0%, respectively), and ultra-pure water (Elga PureUltra, 18.2 MΩ cm, 1 ppb total organic carbon). Argon (Ar, N66) was used to deoxygenate all solutions and CO_2 (BOC) was used to saturate all solutions. Cu(100) and Cu(111) single crystal electrodes from (icryst) were used. Prior to each experiment, the electrodes were prepared by electropolishing in 66% orthophosphoric acid at a voltage of +2 V and, subsequently, rinsing with ultra-pure water. All the measurements have been performed under steady-state conditions and all the voltammograms correspond to the first cycle. The uncompensated solution resistance was measured using the positive feedback mode of the potentiostat and all voltammetries have been corrected by the resistance.

Product characterization by On-line electrochemical mass spectrometry and 1H NMR

On-line Electrochemical Mass Spectrometry (OLEMS) was used to detect the gaseous products formed during the reaction. The reaction products at the electrode interface were collected with a small tip positioned close to the electrode.

NMR samples were prepared by taking 550 µl of the various solutions resulting from the electrochemistry experiments and adding 50 µl of D_2O for lock purposes. We measured the samplesdata on a Bruker AVANCE spectrometer console equipped with a 7T superconducting magnet, operating at a 1H resonance frequency of 400 MHz, fitted with a 5 mm BBO probe and situated in an air-conditioned room. NMR spectra were acquired using a 1D 1H pulse sequence with excitation sculpting and gradients to suppress the water (H_2O) peak.[21] This was optimised on each sample to account for possible small changes in room temperature as well as sample conditions. A spectral width of 11 ppm with 16K complex data points was measured and 1500 scans were acquired for each sample. A delay (d1) of 5 s between scans was used to ensure full signal recovery. The data were processed using TOPSPIN 3.1 software: data were zero-filled to 32k to provide a final spectra resolution of 0.13 Hz per point and spectra were indirectly referenced to TMS at 0 ppm. Further details can be found in the supporting information.

Acknowledgements

MJL acknowledges the University of Birmingham for the financial support through a PhD scholarship at the School of Chemistry. PR would also like to acknowledge the University of Birmingham for financial support through the Birmingham fellowship program.

Keywords: CO_2 reduction • pulse voltammetry • copper electrodes • copper oxides • surface structure • selectivity

1] a) Y. Hori, I. Takahashi, O. Koga, N. Hoshi, *J. Phys. Chem. B* **2002**, *106*, 15-17; b) Y. Hori, in *Modern Aspects of Electrochemistry, Vol. 42* (Eds.: C. Vayenas, R. White, M. Gamboa-Aldeco), Springer New York, **2008**, pp. 89-189; c) A. A. Peterson, F. Abild-Pedersen, F. Studt, J. Rossmeisl, J. K. Nørskov, *Energy Environ. Sci.* **2010**, *3*, 1311; d) J. H. Montoya, A. A. Peterson, J. K. Nørskov, *ChemCatChem* **2013**, *5*, 737-742; e) R. Kas, R. Kortlever, A. Milbrat, M. T. Koper, G. Mul, J. Baltrusaitis, *Phys. Chem. Chem. Phys.* **2014**, *16*, 12194-12201; f) Y. Lee, J. Suntivich, K. J. May, E. E. Perry, Y. Shao-Horn, *J. Phys. Chem. Lett.* **2012**, *3*, 399-404.

[2] a) M. Le, M. Ren, Z. Zhang, P. T. Sprunger, R. L. Kurtz, J. C. Flake, *J. Electrochem. Soc.* **2011**, *158*, E45-E49; b) R. Kortlever, K. H. Tan, Y. Kwon, M. T. M. Koper, *J. Solid State Electrochem.* **2013**, *17*, 1843-1849; c) R. Kas, R. Kortlever, H. Yılmaz, M. T. M. Koper, G. Mul, *ChemElectroChem* **2015**, *2*, 354-358; d) R. Reske, H. Mistry, F. Behafarid, B. Roldan Cuenya, P. Strasser, *J. Am. Chem. Soc.* **2014**, *136*, 6978-6986; e) K. J. P. Schouten, E. Pérez Gallent, M. T. M. Koper, *J. Electroanal. Chem.* **2014**, *716*, 53-57; f) W. Luo, X. Nie, M. J. Janik, A. Asthagiri, *ACS Catal.* **2016**, *6*, 219-229; g) J. Monzó, Y. Malewski, R. Kortlever, F. J. Vidal-Iglesias, J. Solla-Gullón, M. T. M. Koper, P. Rodriguez, *J. Mater. Chem. A* **2015**, *3*, 23690-23698.

[3] F. Calle-Vallejo, M. T. Koper, *Angew. Chem., Int. Ed. Engl.* **2013**, *52*, 7282-7285.

[4] a) Y. G. Kim, J. H. Baricuatro, A. Javier, J. M. Gregoire, M. P. Soriaga, *Langmuir* **2014**, *30*, 15053-15056; b) Y.-G. Kim, A. Javier, J. H. Baricuatro, M. P. Soriaga, *Electrocatalysis* **2016**, *7*, 391-399; c) Y.-G. Kim, A. Javier, J. H. Baricuatro, D. Torelli, K. D. Cummins, C. F. Tsang, J. C. Hemminger, M. P. Soriaga, *J. Electroanal. Chem.* **2016**, *780*, 290-295.

[5] a) A. D. Handoko, C. W. Ong, Y. Huang, Z. G. Lee, L. Lin, G. B. Panetti, B. S. Yeo, *J. Phys. Chem. C* **2016**, *120*, 20058-20067; b) C. W. Li, M. W. Kanan, *J. Am. Chem. Soc.* **2012**, *134*, 7231-7234; c) L. I. Bendavid, E. A. Carter, *J. Phys. Chem. C* **2013**, *117*, 26048-26059.

[6] K. W. Frese, *J. Electrochem. Soc.* **1991**, *138*, 3338.

[7] V. Grozovski, V. Climent, E. Herrero, J. M. Feliu, *Phys. Chem. Chem. Phys.* **2010**, *12*, 8822-8831.

[8] a) D. Friebel, P. Broekmann, K. Wandelt, *Phys. Status Solidi A* **2004**, *201*, 861-869; b) C. Schlaup, S. Horch, *Surface Science* **2013**, *608*, 44-54.

[9] Y. S. Chu, I. K. Robinson, A. A. Gewirth, *J. Chem. Phys.* **1999**, *110*, 5952-5959.

[10] K. J. P. Schouten, E. P. Gallent, M. T. M. Koper, *J. Electroanal. Chem.* **2013**, *699*, 6-9.

[11] a) H. Matsushima, C. Haak, A. Taranovskyy, Y. Grunder, O. M. Magnussen, *Phys. Chem. Chem. Phys.* **2010**, *12*, 13992-13998; b) A. A. Peterson, J. K. Nørskov, *J. Phys. Chem. Lett.* **2012**, *3*, 251-258.

[12] S. Lee, D. Kim, J. Lee, *Angew. Chem., Int. Ed. Engl.* **2015**, *54*, 14701-14705.

[13] R. Kortlever, J. Shen, K. J. P. Schouten, F. Calle-Vallejo, M. T. M. Koper, *J. Phys. Chem. Lett.* **2015**, *6*, 4073-4082.

[14] a) G. C. Chinchen, K. C. Waugh, D. A. Whan, *Appl. Catal.* **1986**, *25*, 101-107; b) G. C. Chinchen, P. J. Denny, D. G. Parker, M. S. Spencer, D. A. Whan, *Appl. Catal.* **1987**, *30*, 333-338.

[15] a) M. Bowker, R. J. Madix, *Surface Science* **1981**, *102*, 542-565; b) M. Bowker, K. C. Waugh, *Surface Science* **2016**, *650*, 93-102.

[16] M. Favaro, H. Xiao, T. Cheng, W. A. Goddard, 3rd, J. Yano, E. J. Crumlin, *Proc. Natl. Acad. Sci. U. S. A.* **2017**, *114*, 6706-6711.

[17] B. J. Cruickshank, D. D. Sneddon, A. A. Gewirth, *Surface Science* **1993**, *281*, L308-L314.

[18] M. R. Vogt, A. Lachenwitzer, O. M. Magnussen, R. J. Behm, *Surface Science* **1998**, *399*, 49-69.

[19] a) M. R. Singh, Y. Kwon, Y. Lum, J. W. Ager, A. T. Bell, *J. Am. Chem. Soc.* **2016**, *138*, 13006-13012; b) J. Resasco, L. D. Chen, E. Clark, C. Tsai, C. Hahn, T. F. Jaramillo, K. Chan, A. T. Bell, *J. Am. Chem. Soc.* **2017**, *139*, 11277-11287; c) M. Liu, Y. Pang, B. Zhang, P. De Luna, O. Voznyy, J. Xu, X. Zheng, C. T. Dinh, F. Fan, C. Cao, F. P. G. de Arquer, T. S. Safaei, A. Mepham, A. Klinkova, E. Kumacheva, T. Filleter, D. Sinton, S. O. Kelley, E. H. Sargent, *Nature* **2016**, *537*, 382-386; d) C. Stoffelsma, P. Rodriguez, G. Garcia, N. Garcia-Araez, D. Strmcnik, N. M. Marković, M. T. M. Koper, *J. Am. Chem. Soc.* **2010**, *132*, 16127-16133.

[20] a) P. Rodriguez, N. Garcia-Araez, M. T. M. Koper, *Phys. Chem. Chem. Phys.* **2010**, *12*, 9373-9380; b) P. Rodriguez, N. Garcia-Araez, A. Koverga, S. Frank, M. T. M. Koper, *Langmuir* **2010**, *26*, 12425-12432; c) P. Rodriguez, Y. Kwon, M. T. M. Koper, *Nat. Chem.* **2012**, *4*, 177-182; d) P. Rodríguez, A. A. Koverga, M. T. M. Koper, *Angew. Chem., Int. Ed.* **2010**, *49*, 1241-1243.

[21] T. L. Hwang, A. J. Shaka, *J. Magn. Reson., Ser. A* **1995**, *112*, 275-279.

Layout 1:

COMMUNICATION

Pulse voltammetry and copper single crystal electrodes were implemented to determine the influence of oxygen species adsorbed on copper electrodes in the electrochemical reduction of CO_2. Product selectivity towards the formation of oxygenated hydrocarbon was associated to the coverage of oxygen species, which is surface-structure-and-potential-dependent.

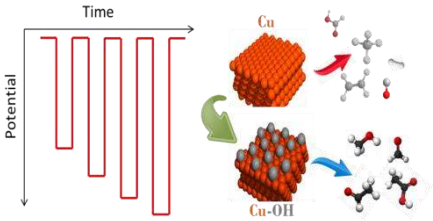

*Cécile S. Le Duff, Matthew J. Lawrence, Paramaconi Rodriguez**

Page No. – Page No.

Role of the adsorbed oxygen species in the selective electrochemical reduction of CO_2 on copper electrodes